

EXPLORING THE HIGH REDSHIFT LARGE-SCALE STRUCTURE OF THE UNIVERSE: A MULTI-WAVELENGTH PERSPECTIVE.

Ivan Valtchanov

*Astrophysics Group, Blackett Laboratory, Imperial College of Science,
Medicine and Technology, London, United Kingdom, e-mail:
i.valtchanov@imperial.ac.uk*

Abstract:

I present a short review of multi-wavelength studies of galaxy clusters and their implications for cosmology and structure formation theories. Some recent results from the XMM Large-Scale Structure Survey are used to illustrate our capability to identify and confirm clusters at high redshifts and to map the large-scale structure out to $z=1$. This allows us, in combination with associated observations in different wavebands, to study the evolution of the structures, to constrain cosmology and to link different aspects of galaxy formation with the environment.

Introducing the main actor – the galaxy clusters

The galaxy clusters are the most massive gravitationally bound objects in the Universe. They are composed of dark matter, gas and galaxies¹. The mass range of clusters is about $10^{14} - 10^{15} M_{\text{sun}}$. The galaxies contribute only about 5% to the total mass, the gas ~15-20% and the rest is dark matter. In general, the different constituents manifest themselves in different regions of the electromagnetic spectrum: the galaxies contribute mainly in the UV, optical and infrared domains, the hot diffuse gas in the X-ray and radio (diffuse radio halo and Syunaev-Zel'dovich effect in the radio mm range) and the dark matter through its effect on the overall cluster dynamics and via the lensing effect. Moreover, the different constituent interact with each other and only by multi-wavelength studies some violent events - like fusion shocks of accretion of galaxy groups infalling into the cluster or gas stripping off the galaxies by their

¹ There is an additional fourth constituent – relativistic particles, mainly electrons at very high energies [14] but they are irrelevant for this review.

interaction with the cluster potential - can be thoroughly studied. It is likely that phenomena like the active galaxy nuclei or bursts of star formation are strongly linked with the environment.

Being the largest virialized entities in the Universe, the galaxy clusters are very rare objects that have arisen from the highest peaks in the primordial density fluctuations. They form at the intersection of the large-scale filamentary structure, grow in mass by accreting gas, individual galaxies and galaxy groups, and trace the large-scale structure as is illustrated in Fig.1.

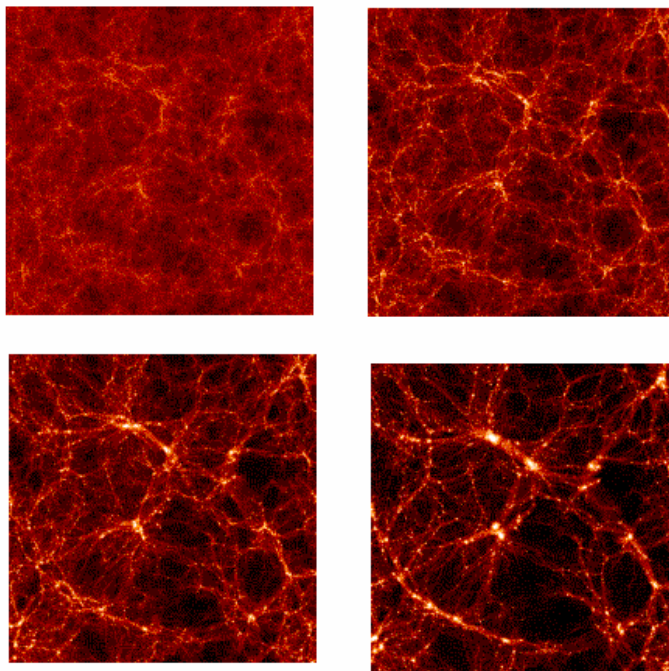


Figure 1. The evolution of 100 Mpc^3 comoving box for LCDM cosmology with dark matter only (no gas). The large-scale structure of the Universe is shown at four different redshifts: $z=5$ (top left), 2 (top right), 1 (bottom left) and present day ($z=0$, bottom right). The galaxy clusters are the bright knots in the intersection of the filamentary structure. Note how they change in contrast from $z=5$ to $z=0$. Simulations R. Teyssier, CEA/Saclay, France.

The number density of clusters as a function of the epoch (or the so called cluster abundance evolution) is very sensitive to the underlying cosmological model, and especially to the normalization of the power spectrum of the density fluctuations σ_8 (the root-mean-square of the density fluctuation in comoving spheres of 8 Mpc/h) and the matter density $\Omega_m = \rho_m/\rho_c$, where ρ_m is the matter density and ρ_c is the critical density of the Universe. Hence, even the counting of clusters as function of redshift could be very important tool in cosmology (see e.g. [12,8]).

The main idea is to compare the observed number of clusters as function of redshift to the expected one for a given set of cosmological models. This can be derived following the Press-Schechter formalism (see e.g. [12] and references therein). An example of the expected cluster abundance evolution for three cosmologies: Λ CDM, OCDM and τ CDM, derived for 64 deg² X-ray cluster survey (see the following Section) is shown in the upper panel of Fig. 2. By constructing sets of cosmological models with different parameters - σ_8 , Ω_m and Γ (the shape parameter of the density fluctuation power spectrum, see e.g. [12]), we can compare the differences between what is observed to what is expected and derive the confidence regions for the parameters, as shown on Fig. 2, lower panels.

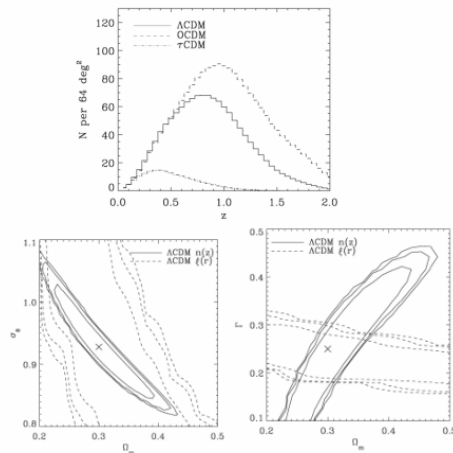


Figure 2. Upper panel: cluster abundance evolution for three cosmologies, derived from the Press-Schechter formalism and calculated for 64

deg² survey. Bottom panels: cosmological constraints on σ_8 , Ω_m and Γ , derived for a reference model and Λ CDM cosmology (see [12] for details).

We must stress that the cosmological constraints derived from the clusters are *independent and complementary* to those from cosmic microwave background (CMB) and supernovae (SNe) studies – the constraints from CMB come from analysis of the temperature fluctuations that arise at the last scattering surface in the early Universe (redshift $z \sim 1000$), while those from SNe rely on the assumption that the supernovae are standard candles. In addition, the galaxy clusters are very important objects because their internal dynamics is a key to the understanding of the evolution of the large-scale structure and the structure formation.

Introducing the scenes: galaxy cluster surveys

In order to use the clusters for cosmological studies or studies of the large-scale structure evolution it is very important that we detect and subsequently confirm clusters and measure different characteristics at the highest possible redshifts. Cluster search in the optical domain is getting very difficult as we go to higher and higher redshift. There are strong projection effects and the galaxy overdensity has very low contrast with respect to the field ([5]). Although there are many optical cluster searches at high redshift (e.g. [11]), which are based on some clever algorithms, the game is rather dubious and difficult. One improvement is to use the diagram colour-magnitude and colour-redshift and search for “red-sequence” of galaxies. This technique is based on the assumption that cluster galaxies have similar colours because they evolve together and the cluster cores contain predominantly elliptical galaxies that evolve passively ([6]). In this way, by choosing convenient colours (for example R-I or V-I or R-z) we can increase the contrast for the cluster galaxy overdensity that can be very successful for redshifts as high as $z \sim 1$ ([1]).

The best way to find clusters, however, is to work in the X-ray domain. Right from the beginning of the X-ray observations of the sky at high galactic latitude, it was realized that one of the most powerful objects were the galaxy clusters ([7]). The thermal X-ray emission is a proof of the existence of a deep potential well, where a diffuse gas ($\sim 10^{-3} \text{ cm}^{-3}$) is trapped and heated by the

gravitation to temperatures $10^7 - 10^8$ K. The X-ray emission measure $S_x \sim n_e^2 \sqrt{T}$ and consequently the projection effects are not important in the X-ray observations of clusters (see e.g. [13] and references therein). Thus, a chance alignment of galaxies cannot give an X-ray emission (no potential well to trap and heat the gas) while it can mistakenly be taken as cluster only based on optical 2D search. In addition, the X-ray sky at high galactic latitudes has two *distinct* types of objects²: super-massive black hole accretion disks (the AGNs), which are point-like unresolved sources and clusters of galaxies, which are extended sources. With the current two great X-ray observatories *Chandra* and *XMM-Newton*, the distinction between these two types of objects is relatively easy.

That is why we have proposed a survey with the XMM-Newton telescope of contiguous region of 64 deg^2 with the main objective to map and study the evolution of the large-scale structure of the Universe traced by the galaxy clusters out to $z \sim 1$. The XMM Large-Scale Structure survey (XMM-LSS) is a combined effort of many astronomical institutes³. A detailed description of the survey may be found in [10,15]; many details are also available from the consortium web pages (see the footnote below).

Briefly, the XMM-LSS survey geometry and depth was chosen such as to allow the study of the cluster-cluster two-point correlation function in the redshift domains $0 < z < 0.5$ and $0.5 < z < 1$ with the same precision as the most precise present day estimation of the correlation scale from the REFLEX survey ([4]) that is based on ROSAT and goes up to $z \sim 0.2$. The placement of the survey was chosen such as to be in a blank area of the sky without known big clusters and no luminous X-ray sources and, from a practical point of view, in equatorial region to allow follow-up as from the northern as well as from the southern hemispheres. The latter is really important because the follow-up programme of such a survey is enormously demanding in terms of telescope time.

² Of course there is some contamination from galactic stars, mainly X-ray binaries, nearby normal galaxies and very rarely supernova remnants.

³ See the official web pages of the consortium:
<http://vela.astro.ulg.ac.be/themes/spatial/xmm/LSS/>

Detailed information on the associated surveys may be found in [10] and updates of the follow-up activities might be found in the official web pages of the consortium.

Cluster detection in XMM-Newton images

To date we have about 6.5 deg^2 observed in X-ray: 55 XMM pointings in total, some with 10 ks exposures and some of 20 ks. The X-ray data were pre-processed with the standard tools from the XMM Science Analysis System (XMM-SAS) to derive calibrated science event lists. The XMM-Newton telescope has three detectors: MOS1, MOS2 and pn which can operate simultaneously or independently. We used the three detectors for our observations and from the resulting event lists we constructed images in different energy bands for each instrument.

The detection pipeline follows the prescription of [16]. Briefly, the images in [0.5-2] keV energy band are combined to increase the signal-to-noise and filtered by multi-scale (wavelet) technique ([14]) using Poisson noise model for the significant wavelet coefficients. The sources on the filtered at 10^{-4} significance level (corresponding to 4σ in Gaussian case) images are then detected and characterised by SExtractor ([2]). Subsequently they are classified to extended (clusters) and point-like (AGNs) using three criteria – a modified stellarity index from SExtractor, full width at half max of the source and the half-light radius. This procedure is very successful at selecting candidate clusters at redshifts even well above 1 (see [16] for details).

An example of an X-ray image in raw photons, from the combined MOS1+MOS2+pn event lists together with adaptively smoothed at signal-to-noise ratio of 5 resulting image are shown on Fig.3. There are two obvious low redshift clusters at $z=0.28$ and $z=0.35$ while the great majority of the remaining sources are AGNs.

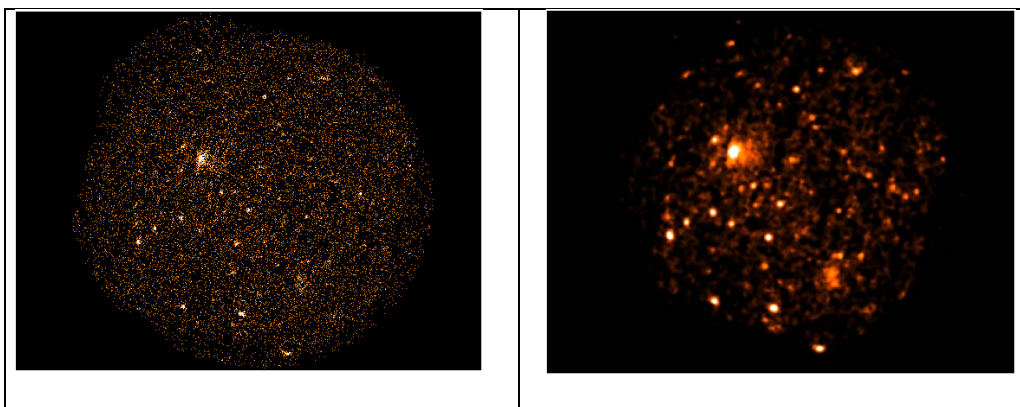


Figure 3. XMM-Newton observation. The left panel shows the raw photon image from the combined photons from the three XMM-Newton detectors MOS1, MOS2 and pn. The diameter of the field is 30 arcmin. The right panel is the adaptively smoothed image from the left panel, with signal-to-noise ratio of 5. Two “low redshift” clusters are obvious (the two extended sources) and the rest of objects are AGNs.

First results from XMM-LSS

Using the above procedure, the list of the detected extended sources is subsequently cross-identified using deep optical images from the CFHT telescope in B, V, R and I bands and all artefacts caused by detector borders were removed. The cluster candidates were divided into classes depending on their photometrical properties: *near* ($z < 0.5$), *mid* ($0.5 < z < 1$) and *dist* ($z > 1$). Depending on the class the candidates were allocated to different observatories for follow-up: 4-m class telescopes (CTIO, ESO-NTT) for *near* candidates; 8-m class telescopes (ESO-VLT) for *mid* and NIR telescopes (NTT-SOFI) for *dist* class.

To date we have undertaken two spectroscopic follow-up runs: fall 2002 and 2003, fall 2004 ESO-VLT (for *mid* and *dist* class) and ESO-NTT (*near*) are underway. Examples of spectroscopically confirmed clusters of each class are shown on Fig. 4. The results on redshifts are summarised on Fig.5.

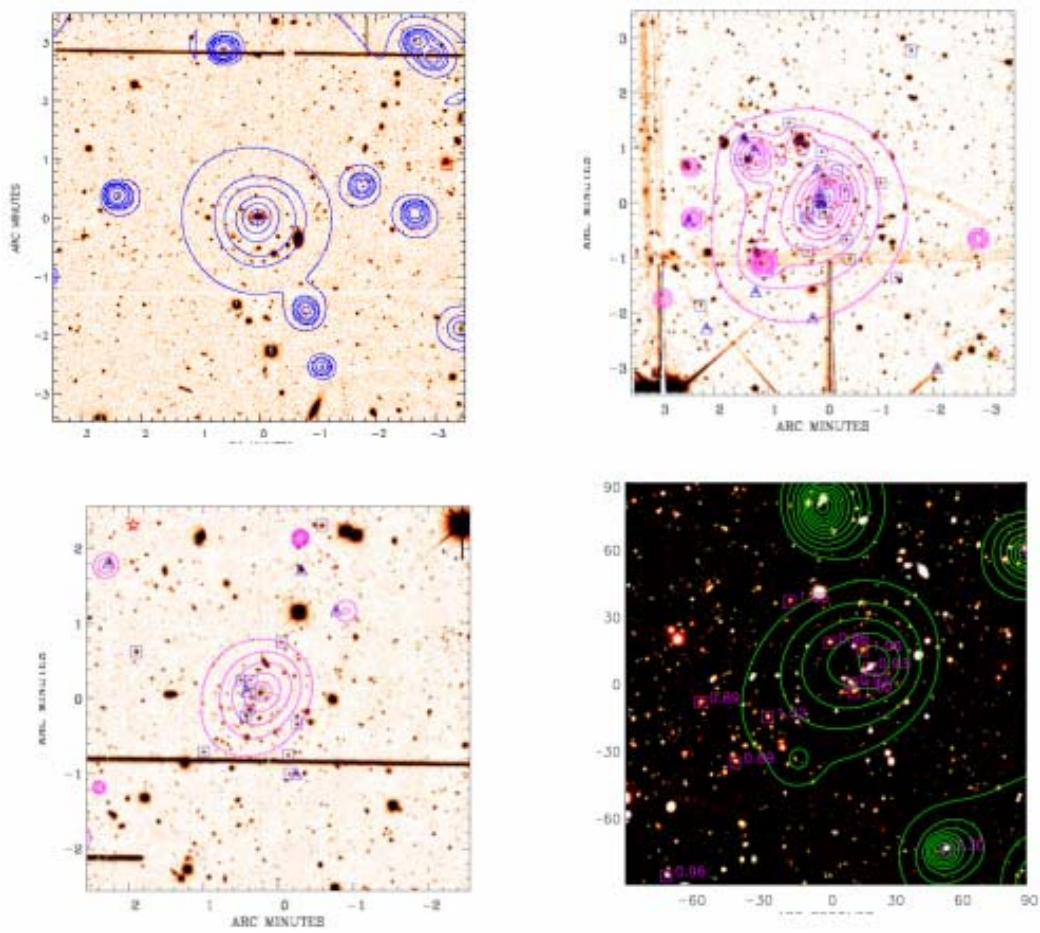


Figure 4. Example of different distance class clusters from the XMM-LSS. A *near* cluster ($z=0.329$, top left panel), a *mid* cluster at $z=0.613$ (top right), *mid* cluster at 0.84 (bottom left) and $z=1$ cluster (bottom right panel).

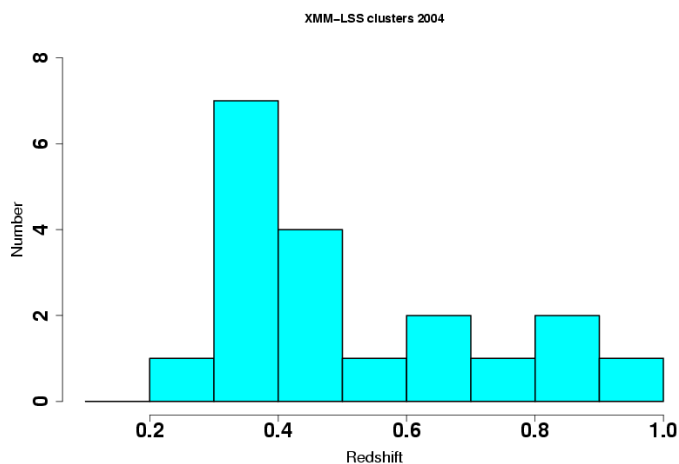


Figure 5. Redshift distribution for all spectroscopically confirmed XMM-LSS clusters for observations performed in 2002 and 2003.

The cluster at $z=1$ is likely to be a superposition of two clusters (see [18]).

The first results of the XMM-LSS, that show the performance of the programme and some exciting new results, are presented in [10,18,19]. Studies of the evolutionary properties of the cluster galaxies from XMM-LSS are presented in [1]. A short summary is presented below and the details may be found in:

- The pipeline procedure is highly efficient: from identification to spectroscopic confirmation we have just one failed objects from 22 candidates and one complicated and interesting case of $z\sim 1$ cluster.
- The number of detected clusters per deg^2 from the first 6.5 deg^2 is consistent with the “concordant” ΛCDM cosmology: ~ 12 clusters per deg^2 out to $z=1$.

- Because of the high efficiency of our programme it was possible for 1h30m VLT time to derive the velocity dispersion of a cluster at $z=0.84$ based on 17 galaxies with concordant redshifts. It is worth to note that to date, there are only 5 known clusters at such high redshift with more than 10 observed galaxy members (3 of them X-ray selected).
- We detect low to moderate mass clusters – a region of the cluster mass function that is largely unexplored and that allows us to map the large-scale structure much densely.
- The combined X-ray identification and NIR observations detected the highest redshift cluster $z = 1.5$ known to date from X-ray observations.

Conclusions and future prospects

Clusters of galaxies are important tools in cosmological studies and in studies of structure and galaxy formations theories. To date the most complete cluster catalogues reach as far as redshift 0.2 and this hampers most of the cosmological applications of clusters. With the advent of the high throughput and high-resolution X-ray observatories like XMM-Newton and Chandra, the detection of clusters at redshifts as high as $z\sim 1$ is possible in systematic manner. This can explain the wealth of X-ray based cluster surveys nowadays, most of which, however, are hunting for high redshift clusters in serendipitous observations (i.e. observations devoted to another object and the cluster happens to lie nearby). This strategy is not very useful for studies of the large-scale structure of the Universe the observations could be scattered all over the sky. Instead, we have proposed a contiguous area X-ray survey with the XMM-Newton telescope – the XMM large-scale structure survey, which can be attained with not so big a demand for observational time. The results of the XMM-LSS, however, will be fundamentally important and impossible for serendipitous clusters even at higher redshift.

The future prospects are all based on routine follow-up of the first 6.5 deg^2 of the XMM-LSS. The highest priority is to get a complete cluster sample from this area, to confirm and place the clusters on the 3-D redshift space, and to use this catalogue following the methodology of [12] to derive cosmological constraints. Another important study is to compare different cluster selection

procedures (optical, colour based, infra-red, X-ray) in order to establish if cluster properties influence the cluster detection.

And finally, the link of galaxy formation with the environment with the Spitzer infra-red observations already acquired from the SWIRE Survey ([9]).

References

- [1] Andreon S., Willis J., Quintana H., et al., 2004, MNRAS, 353, 353
- [2] Bertin E. & Arnouts S., 1996, A&AS, 117, 393
- [3] Borgani, S., Rosati, P., Tozzi, P., et al., 2001, ApJ 561, 13
- [4] Collins C., Guzzo L., Böhringer H. et al., 2000, MNRAS, 319, 939
- [5] Dickinson M., 1997, in *The Early Universe with the VLT*, ed. J. Bergeron, p. 274. Berlin:Springer
- [6] Gladders M. & Yee H., 2000, AJ, 120, 2148
- [7] Gursky H., Kellogg E., Murray S., et al., 1971, ApJ, 167, L81
- [8] Haiman Z., Mohr J. & Holder G., 2001, ApJ, 553, 545
- [9] Lonsdale C. et al., 2003, PASP, 115, 89
- [10] Pierre M., Valtchanov I., Altieri B., 2004, JACP, submitted (astro-ph)
- [11] Postman M., Lubin L., Gunn J., et al., 1996, AJ, 111, 615
- [12] Refregier A., Valtchanov I. & Pierre M., 2002, A&A, 390, 1
- [13] Rosati P., Borgani S. & Norman C., 2002, ARAA, 40, 539
- [14] Sarazin C., 1999, ApJ, 520, 529
- [15] Starck J.-L. & Pierre M., 1998, A&AS, 128, 397
- [16] Valtchanov I. & Pierre M. 2004, AN,
- [17] Valtchanov I., Pierre M. & Gastaud R., 2001, A&A
- [18] Valtchanov I., Pierre M., Willis J., et al., 2004, A&A, 423, 75
- [19] Willis J., Valtchanov I., Pierre M. et al., 2004, A&A, submitted